Synthesis of Ir catalysts featuring amide-functionalized NHC ligands and survey of their activity on formic acid dehydrogenation

Susana García-Abellán,[a] Vincenzo Passarelli[a] and Manuel Iglesias*[a]

[a] S. García-Abellán, Dr Vincenzo Passarelli, Dr Manuel Iglesias
Department of Inorganic Chemistry
Instituto Síntesis Química y Catálisis Homogénea (ISQCH), Universidad de Zaragoza−CSIC
C/ Pedro Cerbuna, 12, Zaragoza, 50009, Spain
E-mail: miglesia@unizar.es

Abstract: 2a and **2b**, [Ir(Cl)(COD)(NHC)] (COD = 1,5-cyclooctadiene), have been prepared via transmetallation from NHC-Ag complexes. [Rh(Cl)(COD)(NHC)] (**4**) was prepared analogously. [Ir({κ-*C*,*N*-(NHC-acetamide–1H)}(COD)] (**3c**) has been synthesized via transmetallation from the deprotonated NHC-Ag complex. [IrCp*({κ-*C*,*N*-(NHC-acetamide–1H)}] (**5**) (Cp* = pentamethylcyclopentadienyl), has been obtained analogously. [Ir(Cl)$(CO)_2$(NHC)] (**6**) and [Ir({κ-*C*,*N*-(NHC-acetamide–1H)}$(CO)_2$] (**7**) have been prepared by carbonylation of **2b** and **3c**, respectively. The catalytic activity of these complexes has been evaluated in the dehydrogenation of formic acid under solventless conditions—with TOF values of 126, 90 and 72 h^{-1} for **2a**, **2b** and **3c**—, in the presence of water as a cosolvent—with TOF values of 445, 298 and 93 h^{-1} for **2a**, **2b** and **3c**—, and in a 5:2 HCOOH/Et_3N mixture—with TOF values of 1940, 1170, 1260, 928 and 777h^{-1} for **2a**, **2b, 3c**, **6** and **7**—. Stoichiometric experiments suggest COD hydrogenation as preactivation step.

Introduction

The use of NHCs (*N*-heterocyclic carbenes) as ancillary ligands in transition metal catalysis has seen great success since the seminal work by Herrmann et al.[1] NHC ligands are strong σ-donors and usually give rise to strong metal-ligand ($M–C_{NHC}$) bonds. Moreover, their umbrella-shaped geometry offers a good steric protection of the metal center.[2] Overall, the electronic and steric properties of NHCs allow for the preparation of stable catalysts that demonstrate remarkable activities in a broad variety of catalytic transformations.

The synthetic flexibility and numerous methodologies so far described for the preparation of NHCs allow the straightforward modification of the wingtip groups and even the nature of the heterocyclic core.[3] This versatility facilitates not only the tuning of their steric and electronic characteristics, but also the introduction of coordinating moieties, leading to the preparation of polydentate architectures.[4] On these grounds, the design of NHCs with substituents capable of triggering metal-ligand cooperation could further improve the catalyst's activity by promoting lower energy pathways. In the case of catalyzed hydrogenation and dehydrogenation reactions, the presence of ligands featuring proton responsive donor groups has proved capable to prompt enhanced activities.[5] An archetypal example of this reactivity is the Noyori-type bifunctional hydrogenation catalyst, wherein the amino moiety of the diamine ligand is able to assist the heterolytic splitting of H_2, as well as the hydride transfer from the metal to the substrate (carbonyl group).[6]

Outer-sphere mechanisms triggered by metal-ligand cooperation play an important role in the homogeneously catalyzed dehydrogenation of formic acid (FA). Remarkably, the proton responsive fragment of the ligand can be coordinated (acting as a chelate) or in the vicinity of the metal center.[7] An interesting example of the former is the bifunctional iridium catalyst reported by Kayaki, based on an amido-amine bidentate ligand scaffold. The proton of the amine moiety was postulated to assist the protonation of the hydride by interaction via hydrogen bonding with a molecule of water (co-solvent), thus promoting the formation of H_2 (Figure 1a).[8] In the case of the latter, a remarkable example is the Ir-PCP catalyst reported by Gelman and Shapiro, where an amino substituent is set in close proximity of the metal center as a result of the steric constrains imposed by the bicyclic structure of the ligand core. This amino moiety directs the β-hydride elimination of the formate, which is the rate-limiting step of the catalytic cycle (Figure 1b).[9]

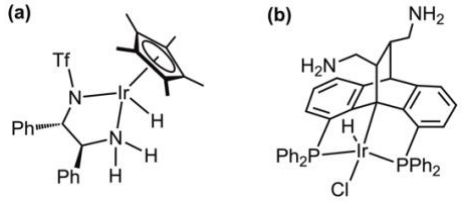

Figure1. Depiction of FADH catalysts reported by Kayaki (a) and Shapiro/Gelman (b).

The impact of these outer-sphere interactions on the reaction mechanism—and, therefore, the activity of the bifunctional catalyst—are subject to the reaction media (e.g., the presence or absence of H_2O as solvent or cosolvent). In this regard, the most commonly explored solvent systems in formic acid dehydrogenation (FADH) are: (i) aqueous solutions, (ii) the 5:2 (molar) HCOOH/Et_3N azeotropic mixture, (iii) organic solvents, and (iv) neat HCOOH. The best TOFs so far reported in aqueous solutions are those described by Li and co-workers with complex [IrClCp*(2,2-bi-2-imidazoline)]Cl (487,500 h^{-1}) at pH 2.8,[10] and the proton-responsive dinuclear Ir catalyst reported by Himeda and Fujita,[11] which operates in a 1M solution of HCO_2H/HCO_2Na (1:1, pH 3.5) (TOF = 228,000 h^{-1}). In the case of HCOOH/Et_3N azeotropic mixtures as reaction media, a TOF of 3630 h^{-1} at 40 °C was achieved with the ruthenium complex [$RuCl_2(DMSO)_4$],[12] and 8500 h^{-1} with the Mn complex [$Mn(CO)_2$(^{tBu}PNNOP)].[13] Noteworthy examples in organic solvents are the Fe-PNP catalyst reported by Hazari and Schneider (TOF = 200,000 h^{-1}),[14] and the Ir(III) catalyst featuring an *N*,*O*-pyridylidene-amine ligand reported by Albrecht (TOF = 280,000 h^{-1}).[15] The dehydrogenation of FA (formic acid) under solventless conditions is of great interest due to the higher energy density of these systems compared to those that employ solvents. However, rather low TOFs have been

reported under these conditions, with the highest values being over 10,000 h^{-1}.[16]

Despite the great success of NHC metal complexes in homogeneous catalysis, reports on ligands based on NHC-scaffolds containing proton responsive fragments are rather scarce.[17] NHC ligands functionalized with acetamide-derived *N*-substituents show promise in the design of bifunctional catalysts.[18] Examples of Pd[19] and Ni[20] complexes have been reported with acetamide-substituted NHC ligands. In this regard, it is worth mentioning that amides have been described to give rise to strong interactions with carboxylic acids via hydrogen bond, even more so than the related homosynthons.[21] Therefore, FA-ligand interactions in acetamide functionalized NHCs are conceivable.

In this work we report on the synthesis and reactivity of a family of iridium-NHC complexes functionalized with acetamide moieties that have the potential to act as bifunctional catalysts. The activity of these catalysts was evaluated in FADH in different reaction media.

Results and Discussion

The NHC precursors, imidazolium salts **1a-c** (Figure 2), 1-(2-methoxyethyl)-3-acetamide-imidazolium iodide, 1-(2-methoxyethyl)-3-acetamide-benzoimidazolium iodide and 1-(2,6-diisopropylphenyl)-3-acetamide-imidazolim iodide, were prepared straightforwardly by quaternization of 1-(2-methoxyethyl)-1H-imidazole, 1-(2-methoxyethyl)-1H-benzimidazole and 1-(2,6-diisopropylphenyl)-1H-imidazole, respectively, with iodoacetamide.

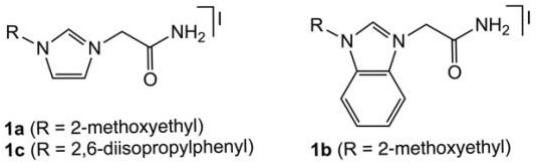

Figure 2. Depiction of imidazolium salts **1a**-**c**.

The crystal structure of **1a** was determined by single crystal X-ray diffraction measurements (see Figure S75 for the molecular structure of **1a** and selected intermolecular contacts).

The synthesis of the [Ir(Cl)(COD)(NHC)] (COD = 1,5-cyclooctadiene) complexes **2a** and **2b** was accomplished by the reaction of imidazolium salts **1a** and **1b** with Ag_2O to afford the corresponding NHC-Ag-Cl complexes, which were reacted *in situ* with $[Ir(\mu\text{-Cl})(COD)]_2$. Conversely, this methodology was unsuccessful in the case **1c**, since protonation of the NHC by the acetamide moiety competes with the transmetallation reaction, thus leading to the formation of **2c** together with the imidazolium salt in ca. 1:1 ratio. Therefore, in order to prevent the protonation pathway, the $-NH_2$ moiety of the **1c[-1H]**-Ag-Cl complex was deprotonated with ^{t}BuOK prior to the reaction with $[Ir(\mu\text{-Cl})(COD)]_2$, thus affording complex **3c** (Scheme 1). This synthetic route was unsuccessful for the preparation of complexes **3a** and **3b**. In the case of the former, an intractable mixture of complexes was obtained, while the latter leads to the formation of **3a** as an unstable complex that decomposes during work up.

Remarkably, the protonation of **3c** with HCl (4M in dioxane) leads to the formation **2c**. At initial reaction times, at room temperature, a mixture of **2c** and a hydride complex is formed. The latter, plausibly being the Ir(III) complex [Ir(Cl)(H){κ-*C*,*N*-(NHC-acetamide)}(COD)], shows a singlet resonance at δ –18.5 ppm in the ^{1}H NMR spectrum. Heating the reaction mixture at 40 °C for 16 h finally results in the formation of **2c** (Scheme 2) together with some impurities that prevented the purification of the complex.

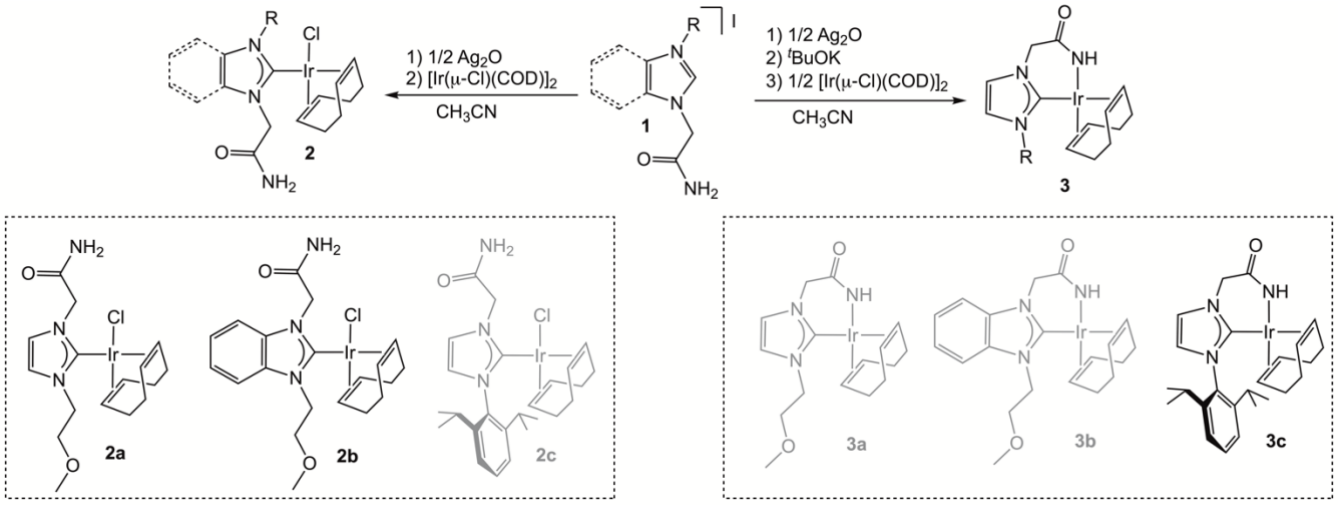

Scheme 1. Synthesis of complexes **2a**, **2b** and **3c**. Complexes in gray (**2c**, **3a** and **3b**) were not prepared successfully by these methodologies.

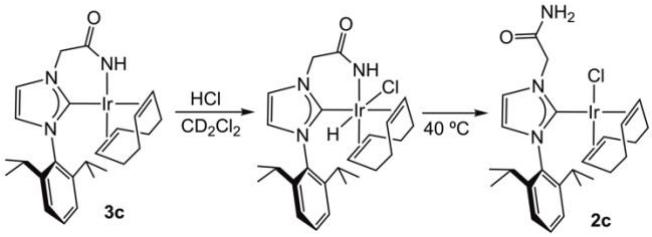

Scheme 2. Synthesis of complex **2c**.

The ^{1}H NMR spectrum of complexes **2a-c** show as diagnostic peaks those of the methylenic and NH_2 protons of the acetamide wingtip group. The methylenic protons appear as two doublets at δ 5.66 and 4.62 ($^2J_{HH}$ = 15.4 Hz), 6.20 and 4.77 ($^2J_{HH}$ = 15.2 Hz), and 5.64 and 5.17 ppm ($^2J_{HH}$ = 15.4 Hz) for **2a**, **2b** and **2c**, respectively. This can be explained in terms of the diastereotopic nature of the CH_2 protons, which is due to the fact that the NHC is perpendicular to the plane of the complex. Consequently, one of the protons of the CH_2 moiety point towards the chloride ligand and the other to the olefin of the COD ligand *trans* to the chloride. The NH_2 moieties of **2a**, **2b** and **2c** give rise to two broad singlets for each proton at δ 6.88 and 5.48, 7.16 and 5.35, and 7.15 and 5.72 ppm, respectively. The most representative resonances in the ^{13}C NMR spectrum are those of the carbene and amide carbons, which appear at δ 180.6 and 191.9 ppm the former, and at δ 169.6 and 169.0 and ppm the latter, for **2a** and **2b**, respectively.

In contrast to complexes **2a-c**, the ^{1}H NMR spectrum of complexes **3c** shows only one broad singlet at δ 5.70 ppm that can be assigned to the NH proton. Moreover, the methylenic protons of the acetamide moiety appear as a singlet at δ 4.53 ppm. The fact that these protons are nor diastereotopic in **3c** strongly suggest *N*-coordination to the metal center, since this constrained geometry would force the CH_2 protons to be above and below the coordination plane of this square planar complex. The same effect is observed for the protons of the isopropyl groups at the diisopropylphenyl substituent. The $CHMe_2$ proton appears as a septuplet ($^3J_{HH}$ = 6.5 Hz) at δ 2.52 ppm in **3c**, while two septuplets at δ 3.35 and 2.18 ppm are observed for **2c**. The ^{13}C NMR spectrum shows the resonances of the carbene and amide carbons at δ 170.7 and 172.1 ppm, respectively.

The FT-IR spectra of the imidazolium salts **1a**, **1b** and **1c** show intense bands at 1667, 1683 and 1683 cm^{-1}, respectively, for the carbonyl groups. These values are close to those obtained for **2a** and **2b**, 1676 and 1691, respectively. In contrast, the FT-IR spectrum of **3c** presents a band at 1589 cm^{-1}, which reveals a weaker C=O bond and further supports amide coordination.

Crystals of **2b** suitable for single-crystal X-ray diffraction analysis were obtained by slow diffusion of hexane into a solution of the complex in dichloromethane. Two nonequivalent molecules of **2b** are present in the unit cell, which will be referred to as **2b** and **2b'**, where the metal center is labeled Ir(1) and Ir(2), respectively. The crystal structures of **2b** and **2b'** confirm the monodentate coordination of the NHC ligand, and a slightly distorted square-planar geometry about the iridium center (Figure 3). The NHC ring is almost perpendicular to the coordination plane, with a torsion angle Cl(1)-Ir(1)-C(1)-N(2) of 88.49° (**2b**), which is the least encumbered arrangement.

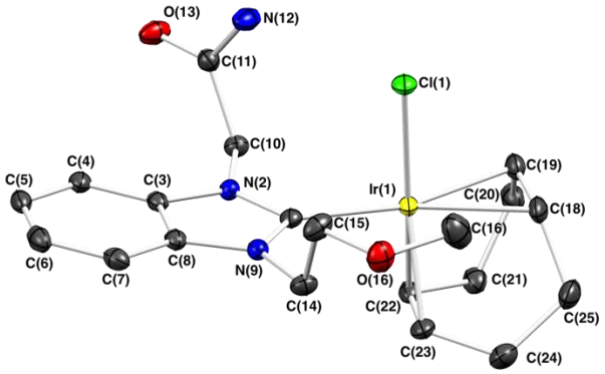

Figure 3. ORTEP view of **2b** (ellipsoids are drawn at the 50% probability level). Hydrogen atoms and a nonequivalent molecule of **2b** co-cristalysed in the unit cell are omitted for clarity. Selected bond lengths (Å) and angles (deg): Ir(1)-C(1) 2.018(3), Ir(1)-C(23) 2.105(3), Ir(1)-C(22) 2.115(3), Ir(1)-C(19) 2.180(3), Ir(1)-C(18) 2.190(3), Ir(1)-Cl(1) 2.3733(7), C(1)-N(9) 1.354(4), C(1)-N(2) 1.366(4); N(9)-C(1)-N(2) 105.8(2), N(9)-C(1)-Ir(1) 127.1(2), N(2)-C(1)-Ir(1) 126.8(2), C(1)-Ir(1)-Cl(1) 87.85(8), C(1)-Ir(1)-ct(2) 93.48, ct(1)-Ir(1)-ct(2) 87.63, C(1)-Ir(1)-ct(2) 93.48, ct(1)-Ir(1)-Cl 91.25. ct(1) and ct(2) are the centroids of the C(18)–C(19) and C(22)–C(23) bonds, respectively.

Remarkably, **2b** features a hydrogen bond between the chloride ligand and the NH moiety of the amide, with a distance Cl(1)-N(12) of 3.328 Å. This allows the second NH bond and the carbonyl oxygen to interact with a second molecule of **2b** via hydrogen bond between the acetamide groups of both molecules, displaying N···O distances of 2.948 Å. In the case of **2b'**, the conformation of the amide wingtip group changes, now pointing away from the chloride ligand. This results in hydrogen bond interactions between the amide group of one molecule and the ether's oxygen atom of the next. The ensuing supramolecular arrangement entails **2b'** forming linear chains via hydrogen bond interactions amide-ether interlocked with dimers formed by amide-amide interactions between molecules of **2b** (Figure 4).

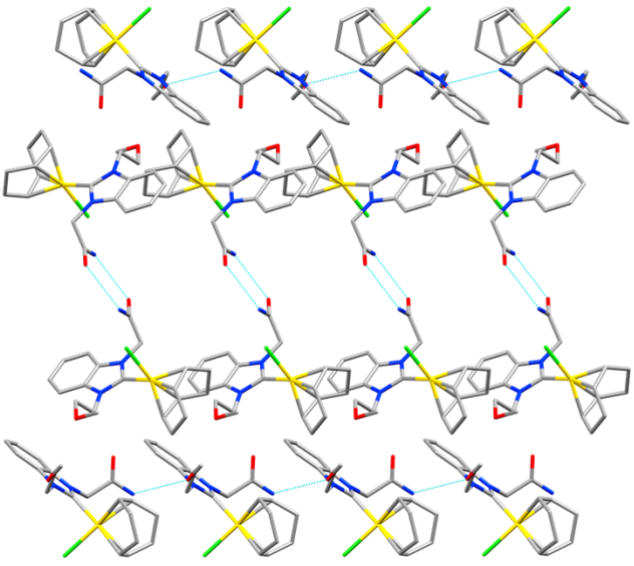

Figure 4. Supramolecular arrangement of **2b** with hydrogen bonds depicted as dotted blue lines.

It is noteworthy that the X-ray crystal structure of the related imidazolium salt **1a** does not show the aforementioned intermolecular interactions due to the presence of the iodide ligand, which interacts via hydrogen bond with the acetamide groups (Figure S75).

In order to allow the comparison of the catalytic activity of the Ir(I) complexes described above with related Rh(I) and Ir(III) complexes, we synthesized [Rh(Cl)(COD){κ-*C*-(NHC-acetamide)}] (**4**) and [IrCp*(Cl){κ-*C*,*N*-(NHC-acetamide)}] (**5**). Complex **4** was prepared by a synthetic procedure analogous to that employed for the related Ir complex **2b**. The ^{1}H and ^{13}C NMR spectra of **4** show no significant difference with those previously described for **2b**. The FT-IR spectrum of **4** is also similar to that of **2b**, presenting a band at 1689 cm^{-1} for the carbonyl bond, which is consistent with a dangling amide moiety.

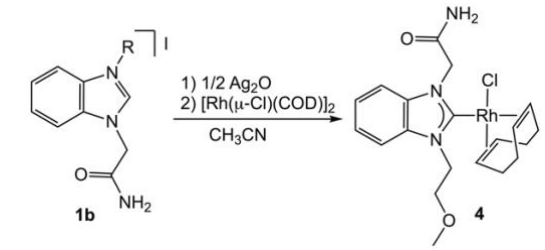

Scheme 3. Synthesis of complex **4**.

The synthesis of **5** was achieved via reaction of the deprotonated silver complex, generated in situ from **1b**, with [IrCp*(Cl)$_2$]$_2$. Noteworthy, direct reaction with the silver complex fails to afford the monodentate NHC-complex, in stark contrast with the reactivity observed for **1b** with [Ir(μ-Cl)(COD)]$_2$. The FT-IR spectrum shows a band at 1594 cm^{-1} that agrees with amide coordination. Diagnostic peaks in the ^{1}H NMR spectrum are the NH proton at δ 4.25 ppm, which appears as a broad singlet, and two doublets at δ 4.62 and 4.46 ppm ($^{2}J_{HH}$ = 15.5 Hz) for the methylenic protons. The ^{13}C NMR spectrum shows resonances of the carbene carbon at δ 170.3 ppm and the carbonyl carbon at δ 169.2 ppm.

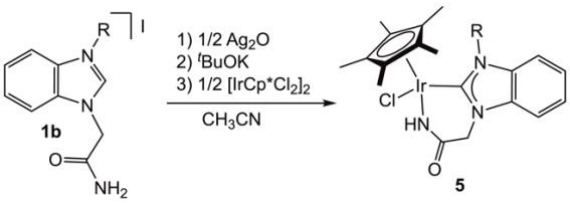

Scheme 4. Synthesis of complex **5**.

Further confirmation for the coordination of the amide moiety in complexes **3c** and **5** was attained by ^{1}H-^{15}N HMQC NMR. The chemical shifts of the salts **1a-c**, which unequivocally present non-coordinated amide moieties, are of δ 102.0 ppm in all cases. Similar shifts were observed for **2a**, **2b, 2c** and **4** (δ 102.0, 100.4, 100.3 and 102.0 ppm, respectively), which indicates that the amide moiety is not coordinated to the metal center. Conversely, complex **3c** presents a δ (^{15}N) of 126.0 ppm, which agrees with the coordination of the amide. An even larger shift was observed for the Ir(III) complex **5** (δ 63.8 ppm), which may account for a stronger Ir–N bond. In addition, in the ^{1}H-^{15}N HMQC NMR spectra of **1a-c**, **2a-c** and **4**, the nitrogen nuclei show two correlations due to the two different protons at the nitrogen atom. In contrasts, in the case of **3c** and **5**, only one correlation is observed, owing to the presence of just one proton.

The complexes described above were tested as catalysts in the dehydrogenation of formic acid. Initially, we evaluated the catalytic activity of complexes **2a**, **2b** and **3c** under solventless conditions, employing a catalyst loading of 0.1 mol%, and a 30 mol% of HCOONa at 80 °C (Figure 5). **2b** showed the best activity (TOF = 126 h^{-1}), followed by **2a** (TOF = 90 h^{-1}), with **3c** being the least active of the three (TOF = 72 h^{-1}). The fact that these complexes show activity in the solventless FADH is noteworthy due to the reduced number of catalysts active under such conditions. However, these values of TOF are modest compared to the most active systems so far reported in the literature.[16] Subsequently, complexes **4** and **5** were studied under analogous conditions, showing no catalytic activity.

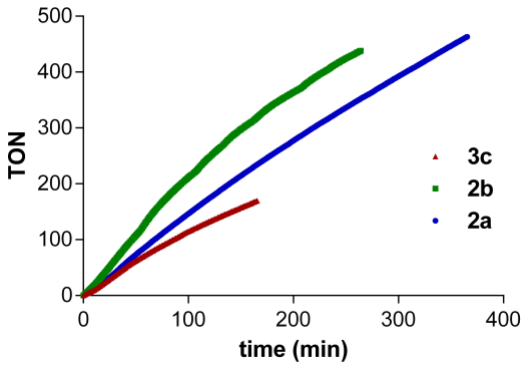

Figure 5. Reaction profiles for the dehydrogenation of FA under solventless conditions (0.1 mol% of the Ir-catalyst and 30 mol% of HCOONa at 80 °C).

The activity of complexes **2a**, **2b** and **3c** was also evaluated in aqueous conditions in a 1:1 HCOOH/H$_2$O mixture, under otherwise analogous conditions to the solventless process. Remarkably, the same activity trend—**2b** (TOF = 445 h^{-1}), **2a** (TOF = 298 h^{-1}), **3c** (TOF = 93 h^{-1})—was observed.

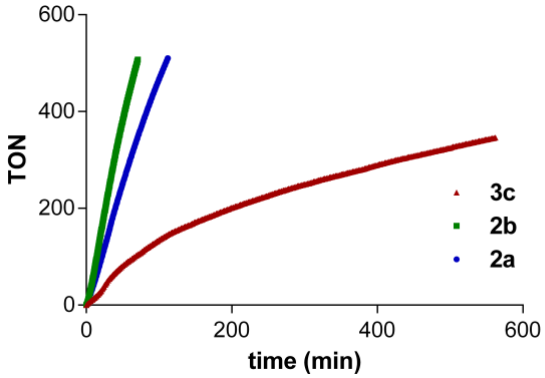

Figure 6. Reaction profiles for the dehydrogenation of FA in a FA/H$_2$O mixture 1:1 in volume (0.1 mol% of the Ir-catalyst and 30 mol% of HCOONa at 80 °C).

The use of water as a cosolvent significantly increases the TOF values observed for **2a** and **2b** under solventless conditions, while

the activity of **3c** experiences only a slight improvement. The Rh complex (**4**), again, shows no activity. The Ir(III) complex **5** displays a good activity at initial reaction times, but it decays quickly, likely due to catalyst deactivation. It is noteworthy that the performance of the catalysts with dangling amide moieties (**2a** and **2b**) experiences a noticeable improvement in the presence of H_2O compared to that featuring the chelating amide (**3c**). This behavior could be attributed to water molecules interacting the with the amide group via hydrogen bond, thus assisting the FADH process; however, this effect, if real, only leads to a marginal improvement of the catalytic activity, resulting in modest TOF values. Other effects could be invoked for the poorer performance of **3c**. First, a preactivation step can be postulated based on the sigmoidal shape of the reaction profile, which would involve a slower hydrogenation of the COD ligand in the case of **3c** compared to **2a** and **2b**. Nonetheless, this does not satisfactorily explain the higher activity observed for **2a** and **2b** at long reaction times. Second, the use of water as a co-solvent could also stabilize unsaturated intermediates formed upon COD hydrogenation. But it is unclear which unsaturated species would benefit more from solvent coordination. Since **2a** and **2b** present a chloride ligand and **3c** a coordinated amide moiety, in principle, the unsaturated species generated from **2a** and **2b** should not require more stabilization than that derived from **3c**.

Finally, we studied the catalytic activity of our complexes in a 5:2 mixture HCOOH/Et_3N employing a 0.1 mol% catalyst loading, which led to a significant improvement of the catalytic activity of complexes **2a** (TOF = 1940 h^{-1}), **2b** (TOF = 1170 h^{-1}) and **3c** (TOF = 1260 h^{-1}). It is noteworthy that the activity trend observed previously under different conditions no longer holds in a 5:2 mixture HCOOH/Et_3N, with **2a** being the most active catalyst in this case. However, it must be noted that, at long reaction times, **3c** performs slightly better than **2a** and **2b**. No significant activity was observed for **4**, while **5** performs substantially worse than **2a**, **2b** or **3c**.

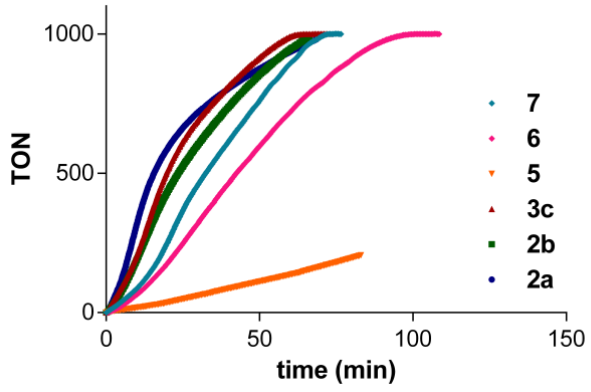

Figure 7. Reaction profiles for the dehydrogenation of FA in a FA/Et_3N mixture 5:2 molar (0.1 mol% of the Ir-catalyst at 80 °C).

Due to the promising reactivity of **2a** and **3c** in a 5:2 mixture HCOOH/Et_3N, we decided to prepare the related biscarbonyl complexes with the intention of exploring their catalytic activity. Note that some Ir-NHC biscarbonyl complexes have shown excellent activities in dehydrogenation reactions;[22] however, deactivation by formation of polyhydride clusters has been described.[23] Thus, **2b** and **3c** were reacted with carbon monoxide under atmospheric pressure at room temperature to afford complexes **6** and **7**, respectively (Scheme 5). The activity of both catalysts was tested in a 5:2 mixture HCOOH/Et_3N, showing significantly lower activities than their parent COD-complexes, with TOF values of 928 and 777 h^{-1} for **6** and **7**, respectively. This reduction of the catalytic activity upon carbonylation may be due to the decrease of the electron density at the metal center in the presence of carbonyl ligands, which would hinder the oxidative addition of the O–H bond of formic acid and, consequently, the activation of the catalyst (Figure 7).[24]

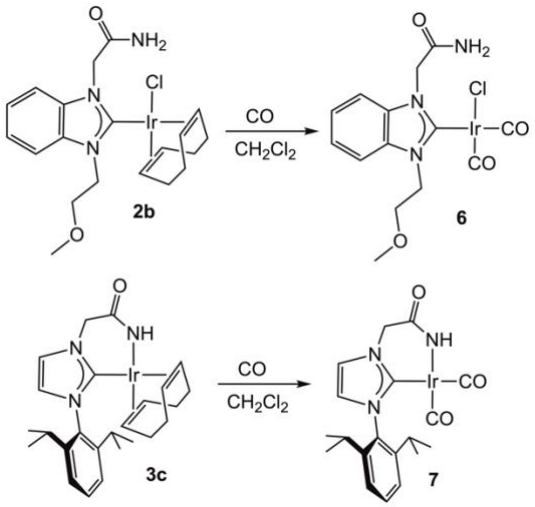

Scheme 5. Synthesis of complexes **6** and **7**.

Stoichiometric experiments in Young NMR tubes were performed in order to gain insight into the nature of the active species. The reaction of **2a** with 4 equiv. of HCOOH in CD_2Cl_2 leads to the incipient formation of a hydride species after 15 min at 50 °C (a singlet at δ –18.1 ppm emerges in the ^{1}H NMR spectrum), but no hydrogenation of the COD ligand to COE or COA is observed. Therefore, this peak can be ascribed to the formation of a hydride complex prior to COD hydrogenation, plausibly the complex [Ir(Cl)(OCHO)(H)(NHC)(COD)]. In fact, the hydride shift (δ –18.1 ppm) is similar to that of the intermediate observed in the protonation of **3c** (δ –18.5 ppm), [Ir(Cl)(H){κ-*C*,*N*-(NHC-acetamide)}(COD)]. At longer reaction times (24 h), after all the HCOOH is consumed, **2a** decomposes to give Ir-particles. Noteworthy, the ^{1}H NMR spectrum of the solution shows the formation of cyclooctane, traces of COE and H_2, which suggests that COD release via hydrogenation takes place,[25,24b] resulting in an unsaturated species that decomposes in the absence of HCOOH. In order to stabilize the proposed unsaturated species, 6 equivalents of pyridine were added to the reaction mixture under otherwise analogous conditions to those described above. This prevents decomposition of **2a**, which allowed us to observe the formation of several hydride species after 16 h at 50 °C, together with the formation of COE and H_2, and the disappearance of the HCOOH peaks. The main species presents a resonance at ca. δ –18 ppm in the ^{1}H NMR, which can plausibly be assigned to a hydride species similar to that proposed above for the reaction without pyridine. Subsequently, we added 16 equiv. of HCOOH and the reaction was subjected to further heating at 50 °C, which

brings about the increase of a peak at δ –27.8 ppm in the ^{1}H NMR spectrum, which becomes the main species at long reaction times (Figure 8). It is noteworthy that, in the presence of a coordinating ligand—namely, pyridine—the catalytic activity persists after total consumption of HCOOH and addition of a new aliquot. These experiments suggest that the formation of the active species requires the hydrogenation of COD to afford an unsaturated hydride complex.

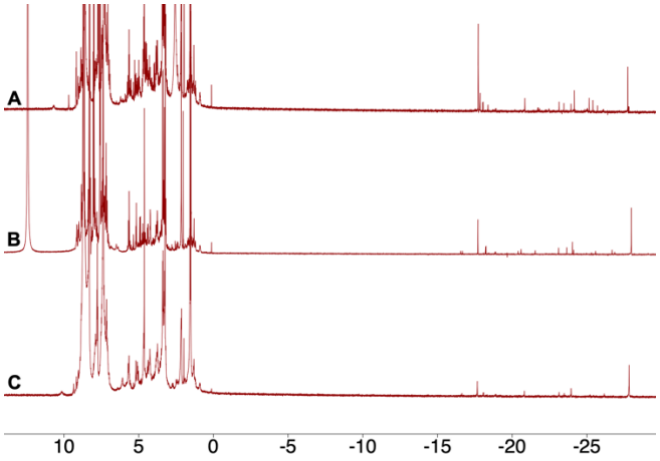

Figure 8. Reaction of **2a** with excess HCOOH in the presence of 6 equiv of pyridine at 50 °C. **A**: 16 h, 4 equiv of HCOOH; **B**: 16 new equiv of HCOOH, 16 h; **C**: 48 h more at 50 °C.

Conclusion

We have developed a convenient method for the preparation of iridium and rhodium complexes that feature a variety of NHC ligands functionalized with an acetamide wingtip group. However, it noteworthy that, in some cases, the transmetallation reaction from silver to iridium results in the protonation of the NHC, thus rendering the imidazolium salt as a by-product. The viability of the transmetallation reaction depends on subtle modifications of the structure of the NHC or even on the nature of the metal precursor. This synthetic conundrum can be circumvented by deprotonating the silver complex before the transmetallation reaction, since the amide's NH_2 moiety is likely the proton source for the protonation of the NHC, thus interfering with the carbene transfer reaction. It must be noted that this reaction successfully affords complexes **3c** and **5**, which present chelating NHC-amide ligands, but the low stability of related complexes **3a** and **3b** prevented their isolation. The NHC-amide complexes prepared in this work were tested as catalysts for the dehydrogenation of formic acid under solventless conditions, in the presence of water as a cosolvent, and in a 5:2 HCOOH/Et_3N mixture. The Rh(I) and the Ir(III) complexes (**4** and **5**, respectively) showed virtually no catalytic activity, while the Ir(I) complexes **2a**, **2b** and **3c** proved active under the different conditions tested here. The use of water as a cosolvent results in an important increase of the activity of **2a** and **2b**, but not **3c**, which might be related with the fact that both feature dangling amide moieties. However, their activity is moderate compared to other literature examples that operate under similar conditions. A more important improvement was observed in the HCOOH/Et_3N mixture, resulting in a TOF_{max} of 1940 h^{-1}, which compares well with literature values. Stoichiometric experiments point to the formation of an unsaturated active species formed by the hydrogenation of the COD ligand, which may decompose in the absence of substrate or a coordinating solvent.

Finally, we believe that the research presented in this manuscript expands the synthetic toolbox for the synthesis of bifunctional catalysts, while also providing significant data to the pre-existing knowledge on this subject.

Experimental Section

General information. All syntheses of organometallic complexes were carried out under an inert atmosphere using the Schlenk technique. The complexes were stored depending on their stability under an inert atmosphere or in a MBraun dry box. The solvents were previously dried and distilled under argon or by means of a solvent purification system (SPS) and collected in an inert atmosphere. All other commercially available starting materials were purchased from Sigma-Aldrich, Merck and J. T. Baker and were used without further purification. The NMR spectra were recorded at 298 K in the Bruker Avance 300 MHz and Bruker Avance 400 MHz spectrometers. Chemical shifts are expressed in ppm and the residual peaks of the solvent were taken as reference. Coupling constants J are given in Hz. Spectral assignments were achieved by combination of ^{1}H-^{1}H COSY, ^{13}C APT, ^{1}H-^{13}C HSQC, ^{1}H-^{13}C HMBC and ^{1}H-^{15}N HMQC experiments. ^{1}H-^{15}N HMQC experiments were recorded with an average J_{N-H} of 80 Hz for direct NH correlations. Attenuated total reflection infrared spectra (ATR-IR) of solid samples were run on a PerkinElmer Spectrum 100 FT-IR spectrometer. High-resolution electrospray mass spectra (HRMS) were acquired using a Bruker MicroTOF-Q hybrid quadrupole time-of-flight spectrometer. 1-(2-methoxyethyl)-1H-imidazole, 1-(2-methoxyethyl)-1H-benzoimidazole and 1-(2,6-diisopropylphenyl)-1H-imidazole were synthesized according to preparations previously described in literature.[26]

Synthesis of 1-carbamoylmethyl-3-methoxiethyl-1H-imidazolim iodide (1a). 1-(2-methoxyethyl)-1H-imidazole (254.4 mg, 2.00 mmol) was dissolved in acetonitrile (7 mL). Subsequently, iodoacetamide (373 mg, 2.00 mmol) was added and the reaction mixture stirred for 16 hours at 80 ºC. After that, the solvent was evaporated under reduced pressure and the resulting orange oil was washed with diethyl ether (3 x 15 mL), obtaining **1a** as a beige solid in an 84% yield (526 mg, 1.68 mmol). ^{1}H NMR (CD_3CN, 400 MHz): δ 8.65 (bs, 1H, NC*H*N), 7.42 (t, J_{H-H} = 1.8, 1H, C*H*$_{Im}$), 7.40 (t, J_{H-H} = 1.8, 1H, C*H*$_{Im}$), 6.75 (bs, 1H, N*H*), 6.13 (bs, 1H, N*H*), 4.96 (s, 2H, NCH_2CO), 4.33 (t, $^{3}J_{H-H}$ = 4.8, 2H, CH_2N), 3.75-3.66 (m, 2H, OCH_2), 3.33 (s, 3H, CH_3O). ^{13}C{^{1}H} NMR APT, ^{1}H-^{13}C HSQC, ^{1}H-^{13}C HMBC (CD_3CN, 101 MHz): δ 167.2 (s, *C*ONH$_2$), 138.1 (s, N*C*HN), 124.6 (s, *C*H$_{Im}$), 123.3 (s, *C*H$_{Im}$), 70.5 (s, OCH$_2$), 59.1 (s, *C*H$_3$O), 51.8 (s, NCH$_2$CO), 50.6 (s, *C*H$_2$N). IR (cm^{-1}, pure sample) 1677 (C=O). HRMS (ESI) Calcd for $[C_8H_{14}N_3O_2]^+$ 184.1086, found 184.1067. ^{1}H-^{15}N HMQC (CD3CN, 400 MHz): δ 102.0 (*N*H$_2$).

Synthesis of 1-carbamoylmethyl-3-methoxiethyl-1H-benzimidazolim iodide (1b). 1-(2-methoxyethyl)-1H-benzoimidazole (528 mg, 3.00 mmol) was dissolved in acetonitrile (7 mL). Subsequently, iodoacetamide (555 mg, 3.00 mmol) was added and the reaction mixture stirred for 16 hours at 80 ºC. After that, the solvent was evaporated under reduced pressure and the resulting orange oil was washed with diethyl ether (3 x 15 mL), obtaining **1b** as an off-white solid in a 74% yield. (806 mg, 2.23 mmol). ^{1}H NMR (CD_3CN, 400 MHz): δ 9.29 (bs, 1H, NC*H*N), 7.94-7.88 (m, 1H, C*H*$_{Ar}$), 7.87-7.81 (m, 1H, C*H*$_{Ar}$), 7.72-7.66 (m, 2H, C*H*$_{Ar}$), 7.02 (bs, 1H, N*H*), 6.27 (bs, 1H, N*H*), 5.31 (s, 2H, NCH_2CO), 4.64 (t, $^{3}J_{H-H}$ = 4.8, 2H, CH_2N), 3.83 (t, $^{3}J_{H-H}$ = 4.8, OCH_2), 3.33 (s, 3H, CH_3O). ^{13}C{^{1}H} NMR APT, ^{1}H-^{13}C HSQC, ^{1}H-^{13}C HMBC (CD_3CN, 101 MHz): δ 167.0 (s, *C*ONH$_2$), 143.6 (s, N*C*HN), 132.8 (s, C_{ipso}N), 132.2 (s, C_{ipso}N), 128.1 (s, *C*H$_{Ar}$), 127.9 (s, *C*H$_{Ar}$), 114.7 (s, *C*H$_{Ar}$), 114.5 (s, *C*H$_{Ar}$), 70.0 (s, OCH$_2$), 59.2 (s, *C*H$_3$O), 49.7 (s, NCH$_2$CO), 48.3 (s, *C*H$_2$N). ^{1}H-^{15}N HMQC (CD_3CN, 400 MHz): δ 102.3 (*N*H$_2$). IR (cm^{-1}, pure sample) 1683 (C=O). HRMS (ESI) Calcd for $[C_{12}H_{16}N_3O_2]^+$ 234.1243, found 234.1237.

Synthesis of 1-carbamoylmethyl-3-(2,6-diisopropylphenyl)-1H-imidazolim iodide (1c). 1-(2,6-diisopropylphenyl)-1H-imidazole (416.7 mg, 1.82 mmol) was dissolved in acetonitrile (7 mL). Subsequently, iodoacetamide (337 mg, 1.82 mmol) was added and the reaction mixture stirred for 16 hours at 80 ºC degrees. After that, the solvent was evaporated under reduced pressure and the resulting orange oil was washed with diethyl ether (3 x 15 mL), obtaining **1c** as a beige solid in 76%yield (572 mg, 1.38 mmol). ^{1}H NMR (CD_3CN, 400 MHz): δ 8.90 (at, J_{H-H} = 1.8, 1H, NC*H*N), 7.71 (at, J_{H-H} = 1.8, 1H, C*H*$_{Im}$), 7.60 (t, $^{3}J_{H-H}$ = 7.9, 1H, C*H*$_{Ar-para}$), 7.53 (at, J_{H-H} = 1.8, 1H, C*H*$_{Im}$), 7.42 (d, $^{3}J_{H-H}$ = 7.8, 2H, C*H*$_{Ar-meta}$), 6.99 (bs, 1H, N*H*), 6.26 (bs, 1H, N*H*), 5.18 (s, 2H, NCH_2CO), 2.37 (hept, $^{3}J_{H-H}$ = 6.9, 2H, C*H*$(CH_3)_2$), 1.17 (d, $^{3}J_{H-H}$ = 6.9, 6H, CH(CH_3)$_2$), 1.16 (d, $^{3}J_{H-H}$ = 6.9, 6H, CH(CH_3)$_2$). ^{13}C{^{1}H} NMR APT, ^{1}H-^{13}C HSQC, ^{1}H-^{13}C HMBC (CD_3CN, 101 MHz): δ 167.1 (s, *C*ONH_2), 146.6 (s, *C*$_{Ar-orto}$), 139.5 (s, NCHN), 132.7 (s, *C*H$_{Ar-para}$), 131.2 (s, *C*$_{ipso}$N), 125.5 (s, *C*H$_{Ar-meta}$), 125.0 (s, *C*H$_{Im}$), 124.4 (s, *C*H$_{Im}$), 52.3 (s, N*C*H_2CO), 29.3 (*C*H$(CH_3)_2$), 24.3 (s, CH(*C*H_3)$_2$), 24.1 (s, CH(*C*H_3)$_2$). ^{1}H-^{15}N HMQC (CD_3CN, 400 MHz): δ 102.0 (*N*H2). IR (cm-1, pure sample) 1683 (C=O). HRMS (ESI) Calcd for $[C_{17}H_{24}N_3O]^+$ 286.1919, found 286.1914.

Synthesis of iridium complex 2a. 1-carbamoylmethyl-3-methoxiethyl-1H-imidazolim iodide (**1a**) (150 mg, 0.48 mmol) was dissolved in acetonitrile (5 mL). Subsequently, Ag_2O (56 mg, 0.24 mmol) was added and the resulting suspension stirred for 2 h protected from light. Then, $[IrCl(COD)]_2$ (162 mg, 0.24 mmol) was added and the reaction stirred for 16 h at room temperature. After that, the reaction mixture was filtered through celite®, the solvent was evaporated under reduced pressure and the resulting yellow oil was washed with diethyl ether (3 x 10 mL), obtaining the yellow complex **2a** as a yellow solid in a 75% yield (187 mg, 0.36 mmol). ^{1}H NMR (CD_2Cl_2, 300 MHz): δ 7.13 (d, $^{3}J_{H-H}$ = 2.0, 1H, C*H*$_{Im}$), 6.97 (d, $^{3}J_{H-H}$ = 2.0, 1H, C*H*$_{Im}$), 6.88 (bs, 1H, N*H*), 5.66 (d, $^{2}J_{H-H}$ = 15.4, 1H, NCH_2CO), 5.48 (bs, 1H, N*H*), 4.69-4.43 (m, 5H, NCH_2CO + C*H*$_{COD}$ + CH_2N), 3.83-3.75 (m, 2H, OCH_2), 3.37 (s, 3H, CH_3O), 3.04-2.97 (m, 1H, C*H*$_{COD}$), 2.96-2.89 (m, 1H, C*H*$_{COD}$), 2.29-2.17 (m, 4H, CH_2 $_{COD}$), 1.81-1.72 (m, 2H, CH_2 $_{COD}$), 1.70-1.61 (m, 2H, CH_2 $_{COD}$). ^{13}C{^{1}H} NMR APT, ^{1}H-^{13}C HSQC, ^{1}H-^{13}C HMBC (CD_2Cl_2, 101 MHz): δ 180.6 (s, N*C*N), 169.6 (s, *C*ONH_2), 123.4 (s, *C*H$_{Im}$), 120.7 (s, *C*H$_{Im}$), 86.4 (s, *C*H$_{COD}$), 85.8 (s, *C*H$_{COD}$), 72.2 (s, OCH$_2$), 59.2 (s, *C*H$_3$O), 54.5 (s, NCH_2CO), 53.1 (s, *C*H$_{COD}$), 52.9 (s, *C*H$_{COD}$), 50.7 (s, *C*H_2N), 33.9 (s, *C*H$_2$ $_{COD}$), 33.8 (s, *C*H$_2$ $_{COD}$), 29.9 (s, *C*H$_2$ $_{COD}$), 29.8 (s, *C*H$_2$ $_{COD}$). ^{1}H-^{15}N HMQC (CD_3CN, 400 MHz): δ 99.5 (*N*H_2). IR (cm^{-1}, pure sample) 1676 (C=O). HRMS (ESI) Calcd for $[C_{16}H_{25}ClIrN_3NaO_2]^+$ 542.1162, found 542.1157.

Synthesis of iridium complex 2b. 1-carbamoylmethyl-3-methoxiethyl-1H-benzimidazolim iodide (**1b**) (100 mg, 0.28 mmol) was dissolved in acetonitrile (5 mL), Ag_2O (32 mg, 0.14 mmol) was added and was stirred for 2 h protected from light. Subsequently, $[IrCl(cod)]_2$ (93.0 mg, 0.14 mmol) was added and the reaction stirred for 16 h at room temperature. After that, the mixture was filtered through celite®, the solvent was evaporated under reduced pressure and the resulting yellow oil was washed with diethyl ether (3 x 10 mL), obtaining **2b** as a yellow solid in an 88% yield (140.6 mg, 0.25 mmol). ^{1}H NMR ($CDCl_3$, 400 MHz): δ 7.55-7.48 (m, 1H, C*H*$_{Ar}$), 7.44-7.39 (m, 1H, C*H*$_{Ar}$), 7.31-7.24 (m, 2H, C*H*$_{Ar}$), 7.16 (bs, 1H, N*H*), 6.20 (d, $^{2}J_{H-H}$ = 15.2, 1H, NCH_2CO), 5.35 (bs, 1H, N*H*), 4.96 (dt, $^{2}J_{H-H}$ = 14.2, $^{3}J_{H-H}$ = 5.2, CH_2N), 4.83-4.74 (m, 4H, NCH_2CO + C*H*$_{COD}$ + CH_2N), 3.97-3.92 (m, 2H, OCH_2), 3.35 (s, 3H, CH_3O), 3.06-3.00 (m, 1H, C*H*$_{COD}$), 2.99-2.94 (m, 1H, C*H*$_{COD}$), 2.34-2.23 (m, 4H, CH_2 $_{COD}$), 1.93-1.82 (m, 2H, CH_2 $_{COD}$), 1.79-1.69 (m, 2H, CH_2 $_{COD}$). ^{13}C{^{1}H} NMR APT, ^{1}H-^{13}C HSQC, ^{1}H-^{13}C HMBC ($CDCl_3$, 101 MHz): δ 191.9 (s, N*C*N), 169.0 (s, *C*ONH_2), 135.8 (s, *C*$_{ipso}$N), 134.3 (s, *C*$_{ipso}$N), 123.5 (s, *C*H$_{Ar}$), 123.5 (s, *C*H$_{Ar}$), 111.4 (s, *C*H$_{Ar}$), 110.4 (s, *C*H$_{Ar}$), 88.9 (s, *C*H$_{COD}$), 88.5 (s, *C*H$_{COD}$), 71.7 (s, OCH$_2$), 59.3 (s, *C*H$_3$O), 53.9 (s, *C*H$_{COD}$), 53.5 (s, *C*H$_{COD}$), 52.7 (s, NCH_2CO), 48.4 (s, *C*H_2N), 33.8 (s, *C*H$_2$ $_{COD}$), 33.8 (s, *C*H$_2$ $_{COD}$), 29.6 (s, *C*H$_2$ $_{COD}$), 29.3 (s, *C*H$_2$ $_{COD}$). ^{1}H-^{15}N HMQC (CD_3CN, 400 MHz): δ 100.0 (*N*H2). IR (cm^{-1}, pure sample) 1691 (C=O). HRMS (ESI) Calcd for $[C_{20}H_{27}ClIrN_3NaO_2]^+$ 592.1319, found 592.1313. Calcd for $[C_{20}H_{27}IrN_3NaO_2]^+$ 534.1733, found 534.1727.

Synthesis of iridium complex 3c. 1-carbamoylmethyl-3-(2,6-diisopropylphenyl)-1H-imidazolim iodide (**1c**) (100 mg, 0.24 mmol) was dissolved in acetonitrile (5 mL), Ag_2O (28.0 mg, 0.12 mmol) was added and was stirred for 24 hours protected from light. After, ^{t}BuOK (30 mg, 0.27 mmol) was added and stirred for 2 h. Then, $[IrCl(COD)]_2$ (81 mg, 0.12 mmol) was added and the reaction was stirred for 16 hours. Subsequently, the solvent was evaporated under reduced pressure, dissolved in dichloromethane and the mixture was filtered through celite®. The solvent was evaporated and the resulting orange oil was washed with diethyl ether (3 x 10 mL), obtaining **3c** as an orange solid in 82% yield (115 mg, 0.20 mmol). ^{1}H NMR (CD_3CN, 400 MHz): δ 7.49 (t, $^{3}J_{H-H}$ = 7.7, 1H, C*H*$_{Ar-para}$), 7.30 (d, $^{3}J_{H-H}$ = 7.7, 2H, C*H*$_{Ar\ meta}$), 7.23 (d, $^{3}J_{H-H}$ = 1.9, 1H, C*H*$_{Im}$), 6.99 (d, $^{3}J_{H-H}$ = 1.9, 1H, C*H*$_{Im}$), 5.70 (bs, 1H, N*H*), 4.53 (s, 2H, NCH_2CO), 3.91-3.84 (m, 2H, C*H*$_{COD}$), 2.68-2.62 (m, 2H, C*H*$_{COD}$), 2.52 (hept, $^{3}J_{H-H}$ = 6.5, 2H, C*H*$(CH_3)_2$), 2.01-1.98 (m, 1H, CH_2 $_{COD}$), 1.81-1.75 (m, 2H, CH_2 $_{COD}$), 1.57-1.46 (m, 5H, CH_2 $_{COD}$), 1.37 (d, $^{3}J_{H-H}$ = 6.9, 6H, CH(CH_3)$_2$), 1.07 (d, $^{3}J_{H-H}$ = 6.9, 6H, CH(CH_3)$_2$). ^{13}C{^{1}H} NMR APT, ^{1}H-^{13}C HSQC, ^{1}H-^{13}C HMBC (CD_3CN, 101 MHz): δ 172.1 (s, *C*ONH), 170.7 (s, N*C*N), 147.3 (s, *C*$_{Ar-orto}$), 136.8 (s, *C*$_{ipso}$N), 131.0 (s, *C*H$_{Ar-para}$), 125.2 (s, *C*H$_{Im}$), 124.7 (s, *C*H$_{Ar-meta}$), 122.8 (s, *C*H$_{Im}$), 80.1 (s, *C*H$_{COD}$), 56.1 (s, NCH_2CO), 55.8 (s, *C*H$_{COD}$), 34.2 (s, *C*H$_2$ COD), 30.0 (s, *C*H$_2$ COD), 29.3 (*C*H$(CH_3)_2$), 25.7 (s, CH(*C*H_3)$_2$), 23.7 (s, CH(*C*H_3)$_2$). ^{1}H-^{15}N HMQC (CD_3CN, 400 MHz): δ 125.9 (*N*H). IR (cm^{-1}, pure sample) 2187(N=C); 1589 (C=O). HRMS (ESI) Calcd for $[C_{25}H_{34}IrN_3NaO]^+$ 608.2229, found 608.2223. Calcd for $[C_{25}H_{35}IrN_3O]^+$ 586.2409, found 586.2404.

Synthesis of iridium complex 4. 1-carbamoylmethyl-3-methoxiethyl-1H-benzimidazolim iodide (**1b**) (75.0 mg, 0.21 mmol) was dissolved in acetonitrile (5 mL). Then, Ag_2O (24.1 mg, 0.10 mmol) was added and the reaction mixture stirred for 2 h protected from light. Subsequently, ^{t}BuOK (26 mg, 0.23 mmol) was added and stirred for 2 h. $[IrCp^*Cl_2]_2$ (83 mg, 0.10 mmol) was then added and the reaction mixture stirred for 16 h at room temperature. Subsequently, the solvent was evaporated under reduced pressure, the crude dissolved in dichloromethane and the resulting mixture filtered through celite®, the solvent was evaporated and the resulting yellow oil was washed with diethyl ether (3 x 10 mL), obtaining **4** as a yellow powder in a 71% yield (88 mg, 0.15 mmol). ^{1}H NMR (CD_3CN, 400 MHz): δ 7.77-7.71 (m, 1H, C*H*Ar), 7.56-7.51 (m, 1H, C*H*$_{Ar}$), 7.34-7.27 (m, 2H, C*H*$_{Ar}$), 4.75-4.68 (m, 1H, C*H*$_2$N), 4.65-4.54 (m, 2H, NCH_2CO + C*H*$_2$N), 4.46 (d, $^{2}J_{H-H}$ = 15.5, 1H, NCH_2CO), 4.25 (bs, 1H, N*H*), 3.91-3.83 (m, 2H, OCH_2), 3.32 (s, 3H, CH_3O), 1.68 (s, 15H, $C_5(CH_3)_5$). ^{13}C{^{1}H} NMR APT, ^{1}H-^{13}C HSQC, ^{1}H-^{13}C HMBC (CD_3CN, 101 MHz): δ 170.3 (s, N*C*N), 169.2 (s, *C*ONH), 135.7 (s, C_{ipso}N), 135.5 (s, C_{ipso}N), 124.3 (s, *C*H$_{Ar}$), 123.8 (s, *C*H$_{Ar}$), 113.4 (s, *C*H$_{Ar}$), 111.2 (s, *C*H$_{Ar}$), 90.8 (s, *C*$_5$(CH$_3$)$_5$), 73.4 (s, OCH$_2$), 59.2 (s, *C*H$_3$O), 50.8 (s, NCH_2CO), 49.6 (s, *C*H_2N), 9.3 (s, C$_5$(*C*H$_3$)$_5$). ^{1}H-^{15}N HMQC (CD_3CN, 400 MHz): δ 67.3 (*N*H). IR (cm^{-1}, pure sample) 2182 (N=C); 1594 (C=O). HRMS (ESI) Calcd for $[C_{22}H_{30}ClIrN_3O_2]^+$ 596.1656, found 596.1650.

Synthesis of rhodium complex 5. 1-carbamoylmethyl-3-methoxiethyl-1H-benzimidazolim iodide (**1b**) (43.3 mg, 0.12 mmol) was dissolved in acetonitrile (5 mL). Then, Ag_2O (14 mg, 0.06 mmol) was added and the resulting suspension stirred for 2 h protected from light. Subsequently, $[RhCl(cod)]_2$ (30 mg, 0.06 mmol) was added and the reaction stirred for 16 h at room temperature. After that, the mixture was filtered through celite®, the solvent was evaporated under reduced pressure and the resulting yellow oil was washed with diethyl ether (3 x 10 mL), to afford **5** as a yellow solid in a 75% yield (45 mg, 0.09 mmol). ^{1}H NMR (CD_3CN, 400 MHz): δ 7.57-7.52 (m, 1H, C*H*$_{Ar}$), 7.35-7.30 (m, 1H, C*H*$_{Ar}$), 7.29-7.22 (m, 2H, C*H*$_{Ar}$), 7.00 (bs, 1H, N*H*), 5.95 (bs, 1H, N*H*), 5.74-5.62 (m, 1H, NCH_2CO), 5.58-5.46 (m, 1H, NCH_2CO), 5.07-4.98 (m, 3H, C*H*$_{COD}$ + CH_2N), 4.92-4.84 (m, 1H, CH_2N), 4.15-4.07 (m, 1H, OCH_2), 4.00-3.93 (m, 1H, OCH_2), 3.57-3.47 (m, 2H, C*H*$_{COD}$), 3.31 (s, 3H, C*H*$_3$O), 2.53-2.36 (m, 4H, CH_2 $_{COD}$), 2.07-1.98 (m, 3H, CH_2 $_{COD}$), 1.84-1.71 (m, 1H, CH_2 $_{COD}$). ^{13}C{^{1}H} NMR APT, ^{1}H-^{13}C HSQC, ^{1}H-^{13}C HMBC (CD_3CN, 101 MHz): δ 198.0 (d, $^{1}J_{Rh-C}$ = 50.3, N*C*N), 170.1 (s, *C*ONH_2), 136.5 (s, *C*$_{ipso}$N), 135.6 (s, *C*$_{ipso}$N), 123.7 (s, *C*H$_{Ar}$), 123.6 (s, *C*H$_{Ar}$), 112.1 (s, *C*H$_{Ar}$), 111.1 (s, *C*H$_{Ar}$), 101.2 (d, $^{1}J_{Rh-C}$ = 45.7, *C*H$_{COD}$), 72.3 (s, OCH$_2$), 70.9 (d, $^{1}J_{Rh-C}$ = 56.2, *C*H$_{COD}$), 59.2 (s, *C*H$_3$O), 52.8 (s, NCH_2CO), 49.1 (s, *C*H_2N), 33.7 (s, *C*H$_2$ $_{COD}$), 33.1 (s, *C*H$_2$ $_{COD}$),

29.6 (s, $CH_{2\ COD}$), 29.2 (s, $CH_{2\ COD}$). ^{1}H-^{15}N HMQC (CD_3CN, 400 MHz): δ 102.0 (*N*H2). IR (cm^{-1}, pure sample) 1689 (C=O). HRMS (ESI) Calcd for $[C_{20}H_{27}ClN_3NaO_2Rh]^+$ 502.0745, found 502.0739.

Synthesis of iridium complex 6. Iridium complex **2b** (100 mg, 0.18 mmol) was dissolved in acetonitrile (5 mL) and stirred for 3 h at room temperature under a CO atmosphere. Instantly, a colour change was observed, from yellow to pale yellow. Subsequently, the CO atmosphere was removed and the solvent was evaporated under reduced pressure. The resulting product was washed with hexane (3 x 4 mL) to afford the pale-yellow complex **6** in a 93% yield (85 mg, 0.16 mmol). ^{1}H NMR ($CDCl_3$, 400 MHz): δ 7.65-7.59 (m, 1H, C*H*$_{Ar}$), 7.57-7.51 (m, 1H, C*H*$_{Ar}$), 7.45-7.38 (m, 2H, C*H*$_{Ar}$), 6.69 (bs, 1H, N*H*), 5.76 (d, $^2J_{H\text{-}H}$ = 15.9, 1H, NC*H*$_2$CO), 5.62 (bs, 1H, N*H*), 5.00-4.86 (m, 2H, NC*H*$_2$CO+ C*H*$_2$N), 4.73-4.63 (m, 1H, C*H*$_2$N), 3.98-3.85 (m, 2H, OC*H*$_2$), 3.32 (s, 3H, C*H*$_3$O), 3.06-3.00. ^{13}C{^{1}H} NMR APT, ^{1}H-^{13}C HSQC, ^{1}H-^{13}C HMBC ($CDCl_3$, 101 MHz): δ 183.6 (s, N*C*N), 180.9 (s, *C*O), 168.0 (s, *C*ONH$_2$), 167.4 (s, *C*O), 135.1 (s, *C*$_{ipso}$N), 134.0 (s, *C*$_{ipso}$N), 124.9 (s, *C*H$_{Ar}$), 124.9 (s, *C*H$_{Ar}$), 112.5 (s, *C*H$_{Ar}$), 111.5 (s, *C*H$_{Ar}$), 71.2 (s, O*C*H$_2$), 59.3 (s, *C*H$_3$O), 52.9 (s, N*C*H$_2$CO), 49.1 (s, *C*H$_2$N). ^{1}H-15N HMQC (CD_3CN, 400 MHz): δ 101.6 (*N*H$_2$). IR (cm^{-1}, pure sample) 2063, 1982 (Ir–CO); 1673 (C=O). HRMS (ESI) Calcd for $[C_{14}H_{15}IrN_3O_4]^+$ 482.0692, found 482.0686.

Synthesis of iridium complex 7. Iridium complex **3c** (100 mg, 0.17 mmol) was dissolved in chloroform (5 mL) and was stirred for 3 h at room temperature under a CO atmosphere. Instantly, a colour change was observed, from orange to pale yellow. Subsequently, the CO atmosphere was removed and the solvent was evaporated under reduced pressure. The resulting product was washed with hexane (3 x 4 mL) to afford the **7** as a pale-yellow solid (80 mg, 0.15 mmol). ^{1}H NMR (CD_3CN, 400 MHz): δ 7.52 (t, ^{3}JH H = 7.8, 1H, C*H*$_{Ar\text{-}para}$), 7.34 (d, $^3J_{H\text{-}H}$ = 7.8, 2H, C*H*$_{Ar\ meta}$), 7.32 (d, $^3J_{H\text{-}H}$ = 1.9, 1H, C*H*$_{Im}$), 7.23 (d, $^3J_{H\text{-}H}$ = 1.9, 1H, C*H*$_{Im}$), 6.40 (bs, 1H, N*H*), 4.71 (s, 2H, NC*H*$_2$CO), 2.50 (hept, $^3J_{H\text{-}H}$ = 6.9, 2H, C*H*(CH$_3$)$_2$), 1.30 (d, $^3J_{H\text{-}H}$ = 6.9, 6H, CH(C*H*$_3$)$_2$), 1.10 (d, $^3J_{H\text{-}H}$ = 6.9, 6H, CH(C*H*$_3$)$_2$). ^{13}C{^{1}H} NMR APT, ^{1}H-^{13}C HSQC, ^{1}H-^{13}C HMBC (CD_3CN, 101 MHz): δ 182.1 (s, *C*O), 176.8 (s, *C*O), 172.7 (s, N*C*N), 171.5 (s, *C*ONH), 147.5 (s, *C*$_{Ar\text{-}orto}$), 136.3 (s, *C*$_{ipso}$N), 131.8 (s, *C*H$_{Ar\text{-}para}$), 125.2 (s, *C*H$_{Ar\text{-}meta}$), 124.9 (s, *C*H$_{Im}$), 124.2 (s, *C*H$_{Im}$), 54.9 (s, NCH$_2$CO), 29.4 (*C*H(CH$_3$)$_2$), 25.2 (s, CH(*C*H$_3$)$_2$), 23.5 (s, CH(CH$_3$)$_2$). ^{1}H-^{15}N HMQC (CD_3CN, 400 MHz): δ 109.2 (*N*H). IR (cm^{-1}, pure sample) 2187 (N=C); 2052, 1976 (Ir–CO); 1603 (C=O). HRMS (ESI) Calcd for $[C_{19}H_{23}IrN_3O_3]^+$ 534.1369, found 534.1363.

Acknowledgements ((optional))

Grants RTI2018-099136-A-I00 and PID2021-126212OB-I00 MCIN/AEI/10.13039/501100011033 funded by "ERDF A way of making Europe", as well as DGA project E42_20R, are gratefully acknowledged. Authors would like to acknowledge the use of "Servicio General de Apoyo a la Investigación-SAI" at the Universidad de Zaragoza and at the ISQCH/CEQMA (CSIC).

Keywords: Carbene • NHC • iridium • formic acid • dehydrogenation

[1] a) W. A. Herrmann, M. Elison, J. Fischer, C. Köcher, G. R. J. Artus, *Angew. Chem. Int. Ed.* **1995**, *34*, 2371–2374; b) F. Glorius, in *N-Heterocyclic Carbenes in Transition Metal Catalysis* (Ed: F. Glorius), Springer, **2007**, Ch 1; c) S. Díez-González, N. Marion, S. P. Nolan, *Chem. Rev.* **2009**, *109*, 3612–3676; d) N. Marion, S. P. Nolan, *Chem. Soc. Rev.* **2008**, *37*, 1776–1782; e) E. A. B. Kantchev, C. J. O'Brien, *Angew. Chem. Int. Ed*. **2007**, *46*, 2768–2813; f) M. Iglesias, L. A. Oro, *Chem. Soc. Rev.* **2018**, *47*, 2772–2808.

[2] A. Gómez-Suárez, D. J. Nelson, S. P. Nolan, *Chem. Commun.* **2017**, *53*, 2650–2660.

[3] a) A. Vivancos, C. Segarra, M. Albrecht, *Chem. Rev.* **2018**, *118*, 9493−9586; b) O. Schuster, L. Yang, H. G. Raubenheimer, M. Albrecht, *Chem. Rev.* **2009**, 109, 3445–3478.

[4] a) R. E. Andrew, L. González-Sebastián, A.B. Chaplin, *Dalton Trans.* **2016**, *45*, 1299–1305; b) Y. Wang, B. Zhang, S. Guo, *Eur. J. Inorg. Chem.* **2021**,188–204.

[5] For examples see: a) R.H. Morris, *Acc. Chem. Res.* **2015**, *48*, 1494−1502; b) T. Zell, David Milstein, *Acc. Chem. Res.* **2015**, *48*, 1979−1994; c) V. Papa, Y. Cao, A. Spannenberg, K. Junge, M. Beller, *Nat. Catal.* **2020**, *3*, 135–142.

[6] P. A. Dub, J. C. Gordon, *Nat. Rev. Chem.* **2018**, *2*, 396–408.

[7] M. Iglesias, L. A. Oro, *Eur. J. Inorg. Chem.* **2018**, 2125–2138.

[8] A. Matsunami, S. Kuwata, Y. Kayaki, *ACS Catal.* **2017**, *7*, 4479−4484.

[9] S. Cohen, V. Borin, I. Schapiro, S. Musa, S. De-Botton, N. V. Belkova, D. Gelman, *ACS Catal.* **2017**, *7*, 8139–8146.

[10] Z. Wang, S.-M. Lu, J. Li, J. Wang, C. Li, *Chem. Eur. J.* **2015**, *21*, 12592−12595.

[11] a) J. F. Hull, Y. Himeda, W.-H. Wang, B. Hashiguchi, R. Periana, D. J. Szalda; J. T. Muckerman, E. Fujita, *Nat. Chem.* **2012**, *4*, 383−388.

[12] D. J. Morris, G. J. Clarkson, M. Wills, *Organometallics* **2009**, *28*, 4133–4140.

[13] N. H. Anderson, J. Boncella, A. M. Tondreau, *Chem. Eur. J.* **2019**, *25*, 10557–10560.

[14] E. A. Bielinski, P. O. Lagaditis, Y. Zhang, B. Q. Mercado, C. Würtele, W. H. Bernskoetter, N. Hazar, S. Schneider, *J. Am. Chem. Soc.* **2014**, *136*, 29, 10234–10237.

[15] N. Lentz, M. Albrecht, *ACS Catal.* **2022**, *12*, 20, 12627–12631.

[16] a) S. Kar, M. Rauch, G. Leitus, Y. Ben-Davis, D. Milstein, *Nat. Catal.* **2021**, *4*, 193–201; b) S. Wang, H. Huang, T. Roisnel, C. Bruneau, C. Fischmeister, *ChemSusChem* **2019**, *12*, 179–184; c) J. J. A. Celaje, Z. Lu, E. A. Kedzie, N. J. Terrile, J. N. Lo, T. J. Williams, *Nat. Commun.* **2016**, *7*, 11308; c) A. Iturmendi, M. Iglesias, J. Munarriz, V. Polo, V. Passarelli, J. J. Pérez-Torrente, L. A. Oro, *Green Chem.* **2018**, *20*, 4875–4879; d) S. Cohen, V. Borin, I. Schapiro, S. Musa, S. De-Botton, N. V. Belkova, D. Gelman, *ACS Catal.* **2017**, *7*, 8139–8146; e) P. Hermosilla, A. Urriolabeitia, M. Iglesias, V. Polo, M. A. Casado, *Inorg. Chem. Front.* **2022**, *9*, 4538–4547.

[17] B. Ramasamy, P. Ghosh, *Eur. J. Inorg. Chem.* **2016**, 1448–1465.

[18] a) M. K. Samantaray, M. M. Shaikh, P. Ghosh, *Organometallics* **2009**, *28*, 2267–2275; b) M. Katari, G. Rajaraman, P. Ghosh, *J. Organomet. Chem.* **2015**, *775*, 109–116.

[19] Y.-C. Lin, H.-H. Hsueh, S. Kanne, L.-K. Chang, F.-C. Liu, I. J. B. Lin, G.-H. Lee, S.-M. Peng, *Organometallics* **2013**, *32*, 3859−3869.

[20] T. V. Roach, M. L. Schmitz, V. A. Leach, M. D. Miller, B. C. Chan, S. E. Kalman, *J. Organomet. Chem.* **2018**, *873*, 8–14.

[21] P. Vishweshwar, A. Nangia, V. M. Lynch, *Cryst. Growth Des.* **2003**, *3*, 5, 783–790.

[22] M. G. Manas, J. Campos, L. S. Sharninghausen, E. Lin, R. H. Crabtree *Green Chem.* **2015**, *17*, 594–600.

[23] a) J. Campos, L. S. Sharninghausen, R. H. Crabtree, D. Balcells, *Angew. Chem. Int. Ed.* **2014**, *53*, 12808 –12811; b) L. S. Sharninghausen, B. Q. Mercado, R. H. Crabtree, D. Balcells, J. Campos, *Dalton Trans.* **2015**, *44*, 18403–18410; c) L. S. Sharninghausen, B. Q. Mercado, C. Hoffmann, X. Wang, J. Campos, R. H. Crabtree, D. Balcells, *J. Organomet. Chem.* **2017**, *849-850*, 17–21.

[24] a) A. Iturmendi, M. Iglesias, J. Munarriz, V. Polo, V. Passarelli, J. J. Pérez-Torrente, L. A. Oro, *Green Chem.* **2018**, *20*, 4875–4879; b) A. Luque-Gómez, S. Garciá-Abellán, J. Munarriz, V. Polo, V. Passarelli, M. Iglesias, *Inorg. Chem.* **2021**, *60*, 15497–15508; c) P. Hermosilla, A. Urriolabeitia, M. Iglesias, V. Polo, M. A. Casado, *Inorg. Chem. Front.* **2022**, *9*, 4538–4547.

[25] Examples were COD release has been proposed: a) P. Kisten, E. Manoury, A. Lledós, A. C. Whitwood, J. M. Lynam, J. M. Slattery, S. B. Duckett, R. Poli, *Dalton Trans.* **2023**, DOI: 10.1039/D2DT04036K; b) A. Iturmendi, N. Garcia, E. A. Jaseer, J. Munarriz, P. J. Sanz Miguel, V. Polo, M. Iglesias, L. A. Oro, *Dalton Trans.* **2016**, *45*, 12835–12845; c) M. V. Jimenez, J. Fernandez-Tornos, J. J. Perez-Torrente, F. J. Modrego, P. Garcia-Orduna, L. A. Oro, *Organometallics* **2015**, *34*, 926–940; d) R.

Spogliarich, J. Kaspar, M. Graziani, F. Morandini, *J. Organomet. Chem.* **1986**, *306*, 407–412.

[26] a) J. Zhou, Y. Liu, Y. Lu, J. Tang and W. Tang, *RSC Adv.* **2014**, *4*, 54512–54516; b) J. Liu, J. Chen, J. Zhao, Y. Zhao, L. Li, H. Zhang, *Synthesis* **2003**, *17*, 2661–2666.